Luo *et al. Journal of Ovarian Research* (2025) 18:269
https://doi.org/10.1186/s13048-025-01856-3

Journal of Ovarian Research

RESEARCH Open Access

hUCMSCs restore ovarian function via angiopoietin 1/2 rebalance in POI rats

Qianqian Luo[1,2†], Chengen Liu[3†], Yongtao Su[4,5*], Ranran Liu[6*] and Zhonglin Jiang[1,7*]

Abstract

Background Premature ovarian insufficiency (POI) is often iatrogenic and the therapeutic potential of human umbilical cord derived mesenchymal stem cells (hUCMSCs) remain incompletely defined. This study aimed to evaluate the effects and underlying mechanism of hUCMSCs on ovarian function in a rat model of POI.

Methods hUCMSCs were characterized by morphology, flow cytometry, and multi-lineage differentiation assays. POI was induced in rats using cyclophosphamide (CTX), followed by intravenous administration of hUCMSCs. Therapeutic outcomes were assessed through cell homing analysis, ovarian histopathology, and serum hormone measurements. Bioinformatic analysis identified Angiopoietin 1 (Angpt1) as a key angiogenic regulator, which was validated by western blot and qRT-PCR. Rat ovarian microvascular endothelial cells (ROMECs) were isolated and functionally assessed under CTX and hUCMSCs treatment using wound healing, tube formation, and evaluation of the Angpt1 and Angpt2 balance.

Results In vivo, hUCMSCs preferentially homed to the ovarian theca layer and restored ovarian function. The Angpt1/Angpt2 ratio was markedly reduced in POI rats but significantly increased after hUCMSCs treatment, and the ratio positively correlated with CD31 expression. In vitro, CTX impaired ROMECs migration and angiogenic capacity, whereas coculture with hUCMSCs rescued these functions and restored the Angpt1/Angpt2 ratio.

Conclusion hUCMSCs ameliorate ovarian dysfunction in POI by modulating the Angpt1/Angpt2 axis, thereby enhancing vascular homeostasis and angiogenesis within the ovarian microenvironment. These findings provided mechanistic insights supporting the clinical translation of hUCMSCs-based therapies for POI.

Keywords Premature ovarian insufficiency, Human umbilical cord mesenchymal stem cells, Rat ovarian microvascular endothelial cells, Angiopoietin 1, Angiopoietin 2

†Qianqian Luo and Chengen Liu contributed equally to this work.

*Correspondence:
Yongtao Su
yongtaosu@126.com
Ranran Liu
ytfylrr@163.com
Zhonglin Jiang
jiangzl21@163.com
[1]Xu Rongxiang Regenerative Medicine Research Center, Binzhou Medical University, Yantai 264003, China
[2]The First Clinical Medical College, Shandong University of Traditional Chinese Medicine, Jinan 250000, China
[3]The Second Clinical Medical College, Binzhou Medical University, Yantai 264003, China
[4]Institute of Drug-Induced Tissue Regeneration and Wound Repair, Shandong University of Traditional Chinese Medicine, Jinan 250000, China
[5]Department of Wound Repair and Plastic Surgery, Affiliated Hospital of Shandong University of Traditional Chinese Medicine, Jinan 250000, China
[6]Department of Medical Laboratory, Yantai Affiliated Hospital of Binzhou Medical University, Yantai 264003, China
[7]Department of Histology and Embryology, College of Basic Medicine, Binzhou Medical University, Yantai 264003, Shandong, China

© The Author(s) 2025. **Open Access** This article is licensed under a Creative Commons Attribution-NonCommercial-NoDerivatives 4.0 International License, which permits any non-commercial use, sharing, distribution and reproduction in any medium or format, as long as you give appropriate credit to the original author(s) and the source, provide a link to the Creative Commons licence, and indicate if you modified the licensed material. You do not have permission under this licence to share adapted material derived from this article or parts of it. The images or other third party material in this article are included in the article's Creative Commons licence, unless indicated otherwise in a credit line to the material. If material is not included in the article's Creative Commons licence and your intended use is not permitted by statutory regulation or exceeds the permitted use, you will need to obtain permission directly from the copyright holder. To view a copy of this licence, visit http://creativecommons.org/licenses/by-nc-nd/4.0/.

Background

Premature ovarian insufficiency (POI) is identified as the cessation of menstruation and ovarian function before 40 years of age in women [1–3]. It is characterized by a persistent decline in follicular number and steroid hormone production, along with deterioration in oocyte quantity and quality [4]. In addition to having a reduced reproductive capacity, POI patients often exhibit a range of endocrine dysfunctions and changes in reproductive organs [5]. POI affects approximately 1% of women, whereas approximately 5% of women experience early menopause before the age of 45 [6, 7].

The pathogenesis of premature ovarian insufficiency (POI) involves multiple mechanisms, including reduced primordial follicle pools at birth and accelerated follicular atresia. Additionally, dysregulated follicular maturation [8–11]. The precise mechanisms of POI remain unclear. Current studies have focused predominantly on granulosa cells (GCs), oocytes, and oocyte-GCs crosstalk, whereas studies on ovarian angiogenesis remain limited [12–15]. Follicular growth critically depends on ovarian vascularization and impaired microvascular endothelial cells can a directly trigger follicular atresia [16, 17].

The angiopoietin (ANGPT) system can modulate endothelial stability through Tie2 receptor activation. ANGPT1 critically influences reproductive angiogenesis and alters ANGPT1 expression in hyperstimulation syndrome [18]. ANGPT2 is an antagonist of TIE2, which constrains vasculature stabilization. In the ovary, ANGPT1 could improve vascular stability via the PI3K/AKT signaling pathway, and its downregulation had been linked to increased follicular atresia [19, 20]. In POI rat models induced by 4-vinylcyclohexene dioxide (VCD), ANGPT2 expression was increased, whereas platelet-rich plasma (PRP) treatment reduced ANGPT2 levels and restored ovarian function [21]. The ANGPT1/ANGPT2 ratio was associated with angiogenesis and follicular development [22, 23]. However, the precise mechanisms underlying the interplay between ANGPT1 and ANGPT2 remain incompletely understood and warrant further investigation.

Currently, the main medications for POI are hormone replacement therapy (HRT), gonadotropin-releasing hormone therapy, and fertility preservation by oocyte cryopreservation [24, 25]. However, these approaches have inherent limitations. Human umbilical cord mesenchymal stem cells (hUCMSCs) have emerged as promising therapeutic options for POI. Previous studies have demonstrated that hUCMSCs can restore ovarian function through apoptosis, ferroptosis and extracellular matrix components [26–29]. However, the precise processes by which hUCMSCs affect angiogenesis and restore ovarian function remain poorly characterized.

This study aimed to investigate the impact of hUCMSCs on ovarian function in a POI rat model on the balance of Angpt1 and Angpt2. The therapeutic potential of hUCMSCs in restoring ovarian function and enhancing angiogenesis via a combination of in vitro and in vivo methodologies will be thoroughly assessed, such as cell culture, immunofluorescence, and gene expression analysis.

Materials and methods

Culture and identification of hUCMSCs

hUCMSCs ($4\times10^4/cm^2$) were obtained from Procell Life Science and Technology Co., Ltd (CP-CL11, Procell, Wuhan) and cultured in low-glucose DMEM supplemented with 10% fetal bovine serum (FBS) and 1% penicillin-streptomycin (PS). The third to fifth passages (P3-P5) of hUCMSCs (4×10^4/ml) were resuspended in PBS and divided into corresponding flow cytometry tubes, with approximately 100 μl of cell suspension added to each tube. Except for the blank control tube, the other tubes were stained with a FITC-labeled mouse anti-human CD73 mAb, a CD90 mAb, a CD44 mAb, and a PE-labeled mouse anti-human HLA-DR mAb, a CD34 mAb, or a CD45 mAb for flow cytometry analysis.

P3 hUCMSCs were seeded in 24-well plates ($6\times10^3/cm^2$). The cells were differentiated in accordance with the directions provided in the adipogenic, osteogenic, and chondrogenic induction kits (PD-017, PD-019, PD-020, Procell, Wuhan). After differentiation, the cells were fixed with 4% paraformaldehyde (PFA) and stained with Oil Red O, Alcian blue, and Alizarin red to observe the differentiation of hUCMSCs into fat, cartilage, and bone cells.

Isolation and culture of rat ovarian microvascular endothelial cells (ROMECs)

ROMECs were isolated from fresh rat ovarian tissues via Percoll density gradient centrifugation (P8370, Solarbio, Beijing). The isolated cells were cultured in endothelial cell medium (CM-ZY001, Procell, Wuhan) under 5% CO_2 and 95% humidity at 37 °C. ROMECs were characterized by morphology and the expression of CD31, Cyp17a1 and FSHR [30, 31].

Construction of the POI rat model and treatment with hUCMSCs

Seven-week-old female Wistar rats were randomly assigned to three groups (n = 25): the control, POI, and POI + hUCMSCs groups. In the control group: the rats were treated with PBS injections; in the POI group, the rats received an initial dosage of cyclophosphamide (CTX) at 50 mg/kg on day 1 (intraperitoneal injection), followed by 8 mg/kg from days 2 to 15. POI + hUCMSCs group: rats received identical dosages of CTX [32, 33].

The rats were then injected via the tail vein with 2×10^6 cells in 200 μl of PBS according to previous studies [26, 29].

After anesthesia with isoflurane, blood samples were collected and incubated overnight before serum separation. The ovaries of the rats were dissected, and the surrounding fat tissue was removed. The ovarian tissues were fixed in 4% PFA for 24 h, dehydrated in a 30% sucrose solution and embedded in optimal cutting temperature (OCT) compound. Using a cryostat, the ovarian tissues were sectioned into 10 μm, five non-serial sections were taken at 100 μm intervals throughout the ovary. Then these slides were kept at room temperature (RT) overnight. After PBS washing, the slices were stained with hematoxylin and eosin. Under the microscope, the morphological structure of ovaries was observed, and growth follicles were only counted when the oocyte nucleus was visible. All morphological and quantitative analyses were performed by an investigator blinded to the group allocations using randomly selected sections from each animal.

In addition, hUCMSCs were labeled with GFP via lentiviral transduction and fluorescence was observed under a fluorescence microscope in frozen sections of rat ovaries at 1, 3, 5, and 7 days to observe their localization.

Immunofluorescence staining

Sections of ovaries were permeabilized and blocked with 10% goat serum albumin for 30 min (RT). Then, the slides were treated with the following primary antibodies: anti-rabbit angiopoietin 1(AF5184, Affinity, 1:100), anti-rabbit angiopoietin 2(DF6137, Affinity, 1:300) and anti-rabbit CD31 (AF6191, Affinity, 1:300) primary antibodies and incubated overnight at 4 °C. Next, the multi-rAb™ CoraLite® Plus 488-Goat anti-rabbit recombinant secondary antibody (H + L) was incubated with the washed sections for 2 h (RT).

ROMECs were fixed in 4% PFA for 15 min at RT. The fixed cells were permeabilized with 0.1% Triton X-100/PBS (15 min, RT) followed by blocking in 10% goat serum (1 h, RT). The cells were incubated with Cytochrome P450 17A1 (AF5210, Affinity, 1:300), anti-rabbit CD31(AF6191, Affinity, 1:300) and anti-FSHR (AF5242, Affinity, 1:300) at 4 °C overnight. After being washed with PBS, the cells were incubated with the multi-rAb™ CoraLite® Plus 488-goat anti-rabbit recombinant secondary antibody (H + L) or goat anti-rabbit IgG (Dylight 549) for 1 h at RT. Finally, the nuclei were counterstained with DAPI (C0065, Solarbio, Beijing) for 5 min and mounted. All the images were observed via the fluorescence microscope. All morphological and quantitative analyses were performed by an investigator blinded to the group allocations using randomly selected sections from each animal. The positive cells for CD31, ANGPT1 and ANGPT2 were quantified in each of these sections, and the results were averaged to obtain a final value per animal.

Enzyme linked immunosorbent assay (ELISA)

The levels of FSH (ml002872, mlbio, Shanghai), E_2 (ml002871, mlbio, Shanghai), LH (ml002286, mlbio, Shanghai) and VEGF (ml002862, mlbio, Shanghai) in the serum samples of each group were determined via ELISA. The serum was diluted 1:4 with ELISA dilution buffer. All the experiments were carried out according to the manufacturer's protocols.

Cell viability assay

The cell viability assay was performed via a CCK-8 kit (BS350B, Biosharp, Anhui) following the manufacturer's instructions. Briefly, ROMECs were seeded in 96-well plates at an optimal density (10,000 cells/well) and incubated for 24 h. Then, medium containing various doses of CTX was added to the ROMECs, and the cells were incubated for another 24 h. Subsequently, 10 μl of the kit reagent was added to each well, and the cells were incubated for an additional 2 h. The absorbance (OD value) was measured at 450 nm utilizing microplate reader.

Tube formation assay

The formation of vessel-like structures was performed in a 96-well plate using Matrix-Gel™ Basement Membrane Matrix (C0371, Beyotime, China) according to established protocols. ROMECs were seeded on extracellular matrix gels and then incubated with CTX and hUCMSCs for 4 h to induce tube formation. Following incubation, capillary-like structures were observed via microscopy. Furthermore, the number of junction sites was quantified to evaluate the capacity of the cells to form tubes.

Wound healing (scratch) assay

Wound healing assays were utilized to quantify cell migration. ROMECs were seeded in 6-well plates until they reached 95% confluence. A uniform scratch was made via sterile pipette tips, and the plates were washed to remove debris. The cells were subsequently treated with CTX and hUCMSCs for 24 h. Images of the wound edges were captured at 0 h and 24 h post scratch using the microscope.

Quantitative Reverse Transcription Polymerase Chain Reaction (qRT-PCR)

Total RNA was extracted from ovarian tissue or cells via FreeZol Reagent (R711-01, Vazyme, Nanjing). The RNA concentration and quality were assessed with a NanoDrop spectrophotometer (Thermo Fisher Scientific, USA). Reverse transcription to cDNA was carried out via the use of HiScript II Q RT SuperMix for qPCR (+ gDNA wiper) (R223-01, Vazyme, Nanjing). The cDNA was then

quantified via qRT-PCR using ChamQ Universal SYBR qPCR Master Mix (Q711-02, Vazyme, Nanjing) on a QuantStudio3 qRT-PCR (Thermo Fisher Scientific, USA). The expression levels of Angpt1, Angpt2 and GAPDH were measured. Relative gene expression was computed via the $2^{-\Delta\Delta Ct}$ method. The specific sequences used are as follows:

Angpt1-F: TGGATGTGAATGGAGGAGGATGG,
Angpt1-R: GTACTGCCTCTGACTGGTTATTGC,
Angpt2-F: AGTGCTGGACATGGAGGACAAG,
Angpt2-R: GCTGCTTCTGAAGGACTGAGTTG,
GAPDH-F: GGCACAGTCAAGGCTGAGAATG,
GAPDH-R: ATGGTGGTGAAGACGCCAGTA.

Western blot

Ovaries or ROMECs were lysed in lysis buffer (E-BC-R327, Elabscience, China) to extract proteins. The protein content was measured via a BCA protein assay kit (PC0020, Solarbio, China). Sodium dodecyl sulfate-polyacrylamide gel electrophoresis (SDS-PAGE) was employed to separate the proteins, which were then transferred onto a PVDF membrane (Millipore, USA). The membrane was blocked with 5% skim milk for one hour and subsequently incubated with primary antibodies overnight at 4 °C. The membranes were subsequently incubated with HRP-conjugated goat anti-rabbit secondary antibodies (1:50000, ZSbio, China) for one hour at room temperature. Images were captured via ECL (Biosharp, China) and analyzed with Image Lab Software (Bio-Rad, USA). The primary antibodies used for Western blotting were against CD31(AF6191, Affinity), Angpt1 (AF5184, Affinity), Angpt2 (AF5124, Affinity) and GAPDH (AF7021, Affinity). All the antibodies were diluted according to the provided instructions.

Bioinformatic identification of Angiogenesis-Associated genes in POI

The gene expression dataset GSE39501 was retrieved from the Gene Expression Omnibus (GEO) and contains ovarian tissue samples from 3 mice with POI and 3 controls. Differential expression analysis was performed via GEO2R. Significantly differential expressed genes (DEGs) with P values < 0.05 were identified.

To investigate the mechanism of POI pathogenesis, curated gene lists related to angiogenesis, POI and cell migration were extracted from the GeneCards database and transferred to homologous mouse genes. A Venn diagram was generated to discover overlapping genes. A protein-protein interaction (PPI) network was subsequently constructed with the STRING database (V11.5, confidence score = 0.4), and key module genes were identified via the MCODE plug-in Cytoscape (v3.9.1). The expression of key module genes is shown via a box plot.

Statistical analysis

Target and reference proteins were quantified via ImageJ software (National Institutes of Health, USA). The relative expression of the target proteins was normalized to the reference value and represented as the mean ± standard deviation (SD) via SPSS 20 software. The normality of data distribution and homogeneity of variances were verified using the Shapiro-Wilk test and Levene's test, respectively. Multiple samples were compared via one-way ANOVA followed by the least significant difference (LSD) method. The statistically significant threshold was set at a P value < 0.05.

Results

Differentiation and phenotypic identification of hUCMSCs

hUCMSCs adhered to the culture plates and presented a distinctive spindle-shaped, fibroblast-like morphology that was consistent with the identities of mesenchymal stem cells (MSCs) (Fig. 1A). Under differentiation conditions, hUCMSCs effectively developed into osteoblasts, adipocytes, and chondrocytes, as confirmed by Alizarin Red, Oil Red O, and Alcian blue staining, respectively (Fig. 1B-D). Flow cytometry analysis revealed that these cells were highly positive for the classical MSCs surface markers CD44, CD90, and CD73 but negative for CD45, CD34 and HLA-DR (Fig. 1E). These results are consistent with our previous studies, which demonstrated that hUCMSCs were successfully identified [28].

hUCMSCs improves ovarian function in POI rats

To assist in tracking, hUCMSCs were tagged with green fluorescent protein (GFP) via a lentivirus. The findings were presented in Fig. S1. GFP-labeled hUCMSCs were injected via the tail vein, and fluorescence was observed at 1, 3, 5, and 7 days in the rat ovaries (Fig. 2A). The results suggested that hUCMSCs-GFP progressively migrated to the follicle theca layers over time. Compared with those of the control group, the body and ovary weights of the POI rats were lower (Control vs. POI: body weight: $P = 0.000$; ovary weights: $P = 0.011$). Following treatment with hUCMSCs, these parameters dramatically increased (Fig. 2B, C) (POI vs. POI + hUCMSCs: body weight: $P = 0.002$; ovary weights: $P = 0.029$). Hematoxylin-eosin staining revealed that POI rats developed follicular depletion, including primary and *secondary* follicle depletion. hUCMSCs therapy restored follicular counts (Number of growing follicles: Control vs. POI: $P = 0.005$; POI vs. POI + hUCMSCs: $P = 0.001$). Compared with the Control group, the POI group presented lower had estradiol (E_2) levels and significantly elevated follicle-stimulating hormone (FSH) and luteinizing hormone (LH) levels, with a notable decrease in vascular endothelial growth factor (VEGF) levels (Control vs. POI: E_2: $P = 0.002$; FSH: $P = 0.013$; LH: $P = 0.000$; VEGF: $P = 0.006$).

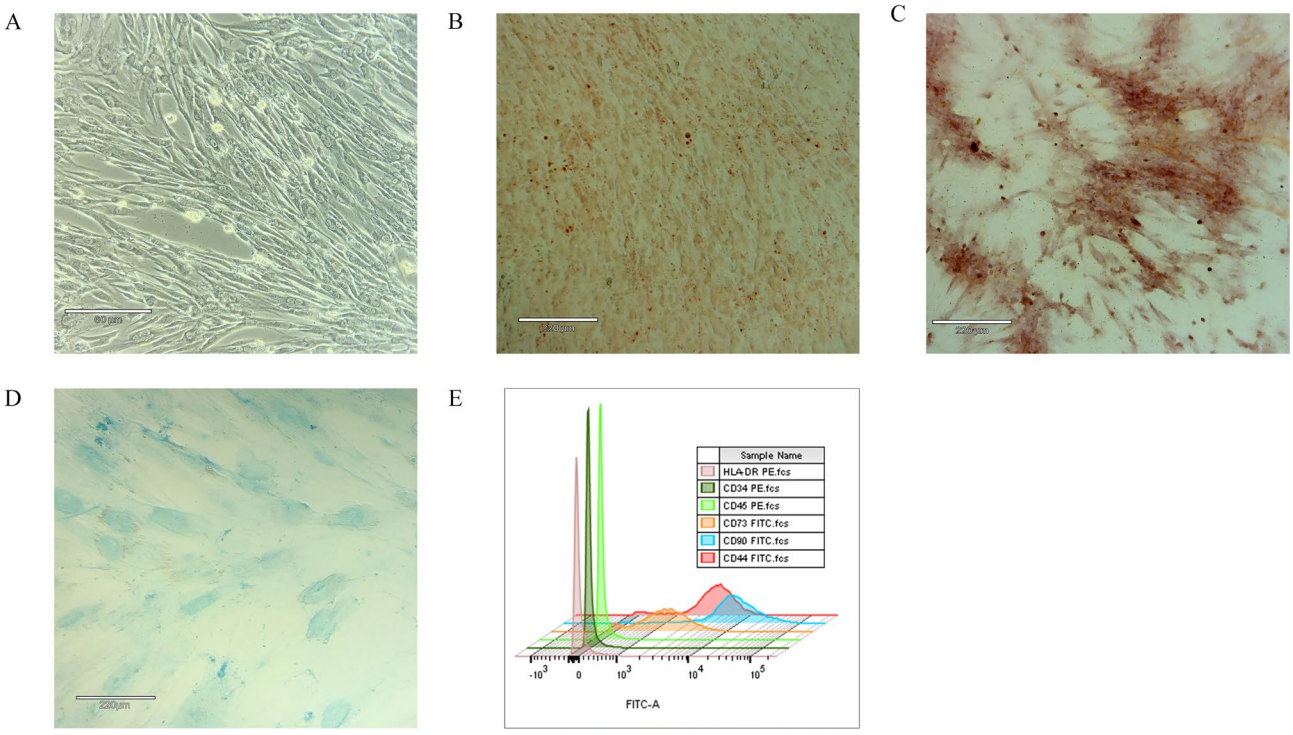


Fig. 1 Differentiation and Immunophenotypic Identification of hUCMSCs. (**A**) The morphology of hUCMSCs showing typical fibroblast-like phenotype (40×). (**B**) Adipogenic differentiation evidenced by Oil Red O staining (100×). (**C**) Alizarin Red staining verifying the osteoblasts differentiation (100×). (**D**) Chondrogenic differentiation with Alcian Blue staining (100×). (**E**) Immunophenotypic identification of hUCMSCs

After hUCMSCs treatment, the serum E_2 level increased significantly, while the FSH and LH levels decreased, and the VEGF level increased substantially (Fig. 2F-I) (POI vs. POI + hUCMSCs: E_2: $P = 0.043$; FSH: $P = 0.022$; LH: $P = 0.000$; VEGF: $P = 0.015$). These data revealed that the POI rat model was successfully established and that hUCMSCs effectively restored ovarian function in POI rats.

hUCMSCs potentially affect vascular generation

Previous data confirmed that hUCMSCs localize to the theca layers which are regions populated with microvasculature, and the expression of CD31, an angiogenesis marker, was quantitatively assessed. Immunofluorescence analysis revealed that the fluorescence signals of CD31 considerably decreased in the POI model and improved after hUCMSCs therapy (Fig. 4A). Western blot analysis revealed similar results. The protein expression of CD31 was reduced in POI ovaries; however, this effect was reversed following hUCMSCs therapy (Fig. 4B, C) (CD31 expression: Control vs. POI: $P = 0.01$; POI vs. POI + hUCMSCs: $P = 0.017$). These data gathered suggest that hUCMSCs might promote vascular generation in the ovaries of POI rats.

Bioinformatics analysis revealed that the ratio of Angpt1 to Angpt2 affects angiogenesis in POI

To further study the mechanism of angiogenesis implicated in POI, data analysis was performed on GSE39501 and UMAP revealed distinct clustering between POI and control samples, which suggested that this dataset was appropriate for downstream analysis (Fig. 3A). Using GEO2R, we identified differentially expressed genes (DEGs). Intersection analysis with gene lists from GeneCards (angiogenesis, premature ovarian insufficiency and cell migration) and DEGs yielded 199 POI-related angiogenesis genes (Fig. 3B). The heatmap showed the expression patterns of those overlapping DEGs (Fig. 3C). Protein-protein interaction networks were constructed via the String database, and the key module was identified via the MCODE plug-in to identify important genes (Fig. 3D, E). Based on previous studies, we focused on Angpt1 and Angpt2, which contribute to angiogenesis. The expression of Angpt1 and Angpt2 was displayed via a box plot (Fig. 3F), Angpt1 expression tended to decrease, whereas Angpt2 expression did not differ. On the basis of these findings, we suggest that the ratio of Angpt1 to Angpt2 might be involved in the progression of POI.

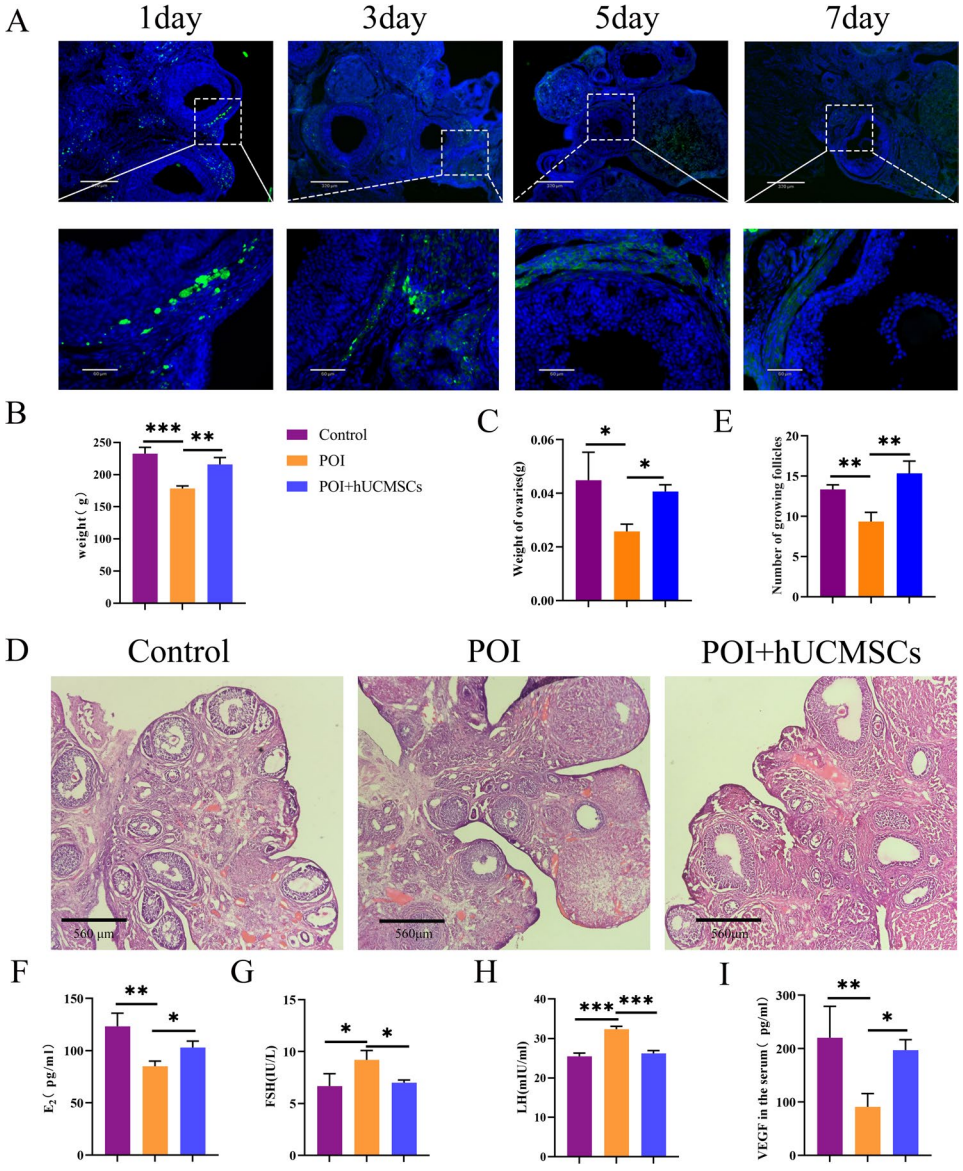


Fig. 2 Therapeutic effects of hUCMSCs on ovarian structure and endocrine function in POI rat models. **A** GFP-labeled hUCMSCs homing to the theca layer. (200×, 400×) (**B**) Body weight of rats among groups. **C** The weight of ovarian across experimental groups. **D** HE staining to observe rats' ovarian morphology (40×). **E** The number of growing follicles in ovarian tissues. **F**-**I**. Concentration of E_2, LH, FSH, and VEGF. E_2: Estradiol; LH: Luteinizing hormone; FSH: Follicle-stimulating hormone; VEGF: Vascular endothelial growth factor. Data were shown as mean ± SD of at least three independent experiments. *: $P<0.05$, **: $P<0.01$, ***: $P<0.001$

hUCMSCs alleviated the ratio of Angpt1 to Angpt2 in ovaries

We used Immunofluorescence, Western Blot and qRT-PCR to further explore whether hUCMSCs could regulate the balance between Angpt1 and Angpt2 to influence angiogenesis in the ovaries. Immunofluorescence analysis revealed that the Angpt1 signal was reduced in the POI group and improved following hUCMSCs therapy. Conversely, the fluorescence signal of Angpt2 remained unchanged across the groups (Fig. 4A). The results of both Western blot and qRT-PCR revealed that the expression of Angpt1 was lower in POI ovaries than in control ovaries and that hUCMSCs treatment restored Angpt1 expression (Control vs. POI: Angpt1 expression: $P=0.005$, Angpt1 mRNA expression: $P=0.000$; POI vs. POI + hUCMSCs: Angpt1 expression: $P=0.036$, Angpt1 mRNA expression: $P=0.000$). However, the expression of Angpt2 did not significantly differ between the three groups (Fig. 4B, E-F, H-I) (Control vs. POI: Angpt2 expression: $P=0.905$, Angpt2 mRNA expression: $P=0.915$; POI vs. POI + hUCMSCs: Angpt1 expression: $P=0.932$, Angpt1 mRNA expression: $P=0.568$). Thus, there were an Angpt1/Angpt2 imbalance in POI, and hUCMSCs recovered this ratio (Fig. 4G, J) (Control

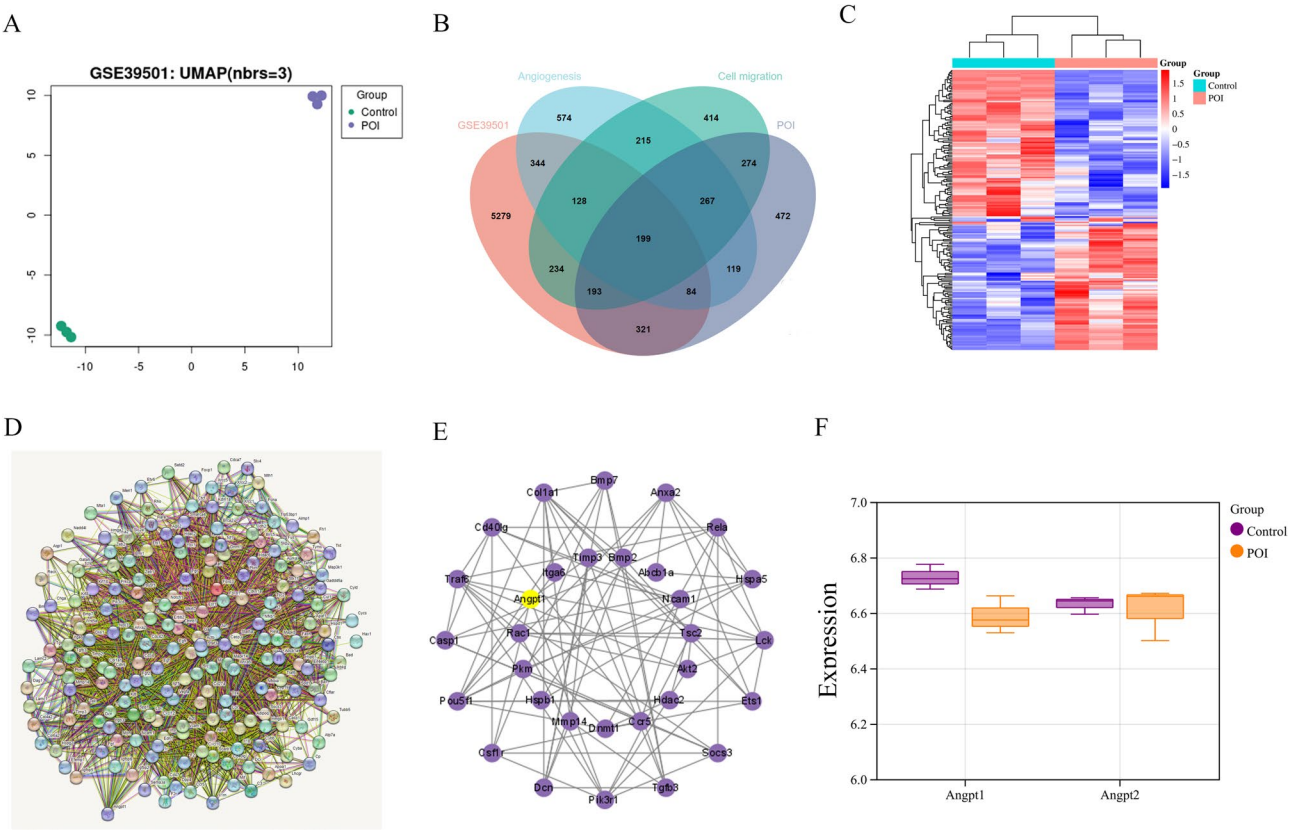


Fig. 3 Bioinformatics analysis screened angiogenesis genes in POI. **A** Umap visualization of sample distribution. **B** DEGs intersection with angiogenesis, POI and cell migration. **C** Heatmap of overlapping genes expression profiles. **D** PPI networks construction for overlapping DEGs. **E** Hub module identification via MCODE. **F** The expression of Angpt1 and Angpt2 in datasets

vs. POI: Angpt1/Angpt2 ratio: $P = 0.003$, Angpt1/Angpt2 ratio (mRNA): $P = 0.000$; POI vs. POI + hUCMSCs: Angpt1/Angpt2 ratio: $P = 0.037$, Angpt1/Angpt2 ratio (mRNA): $P = 0.001$). Crucially, we identified a strong positive correlation between the Angpt1/Angpt2 ratio and CD31 (Fig. 7D) ($P = 0.004$). These findings demonstrated that hUCMSCs rebalanced the Angpt1/Angpt2 ratio, which directly promoted microvascular regeneration.

Identification of ROMECs

Primary ROMECs were isolated from fresh rat ovarian tissues as described previously. The isolated cells displayed a fibroblast-like morphology and a typical endothelial-like cobblestone morphology (Fig. 5A). Furthermore, the immunofluorescence results revealed that the expression of CD31 in ROMECs was positive, whereas the expression of FSHR and Cyp17a1 was negative (Fig. 5C). P3 ROMECs were used for tube formation assays, and the formation of tubular structures was observed (Fig. 5D). Collectively, these results indicated that ROMECs were successfully isolated and cultured.

The CCK-8 assay was used to determine the optimal cytotoxic concentration of CTX for ROMECs, revealing a concentration-dependent decrease in cell viability. On the basis of these results, subsequent experiments utilized 80 μM CTX for 24 h (Fig. 5B) (Cell viability: 0μM vs. 5 μM: $P = 1$; 0μM vs. 10 μM: $P = 0.472$; 0μM vs. 20 μM: $P = 1$; 0μM vs. 30 μM: $P = 1$; 0μM vs. 40 μM: $P = 1$; 0μM vs. 50 μM: $P = 0.707$; 0μM vs. 60 μM: $P = 0.564$; 0μM vs. 70 μM: $P = 0.135$; 0μM vs. 80 μM: $P = 0.024$; 0μM vs. 90 μM: $P = 0.000$).

hUCMSCs restore angiogenesis in ROMECs through the Angpt1/Angpt2 axis

Tube-forming and scratch experiments were employed to explore the effects of hUCMSCs on the tube formation and migration of ROMECs. The results of tube formation experiments revealed that ROMECs formed fewer tube lumen structures in the CTX group than in the control group, whereas hUCMSCs treatment significantly increased tubulogenesis (Fig. 6A, C) (Number of junction points: Control vs. POI: $P = 0.001$; POI vs. POI + hUCMSCs: $P = 0.002$). Similarly, a scratch experiment revealed that CTX inhibited ROMECs migration after 24 h, whereas hUCMSCs markedly promoted cell migration (Fig. 6B, D) (Scratch clousure rate: Control vs. POI: $P = 0.000$; POI vs. POI + hUCMSCs: $P = 0.024$). The in vitro experiments demonstrated that hUCMSCs

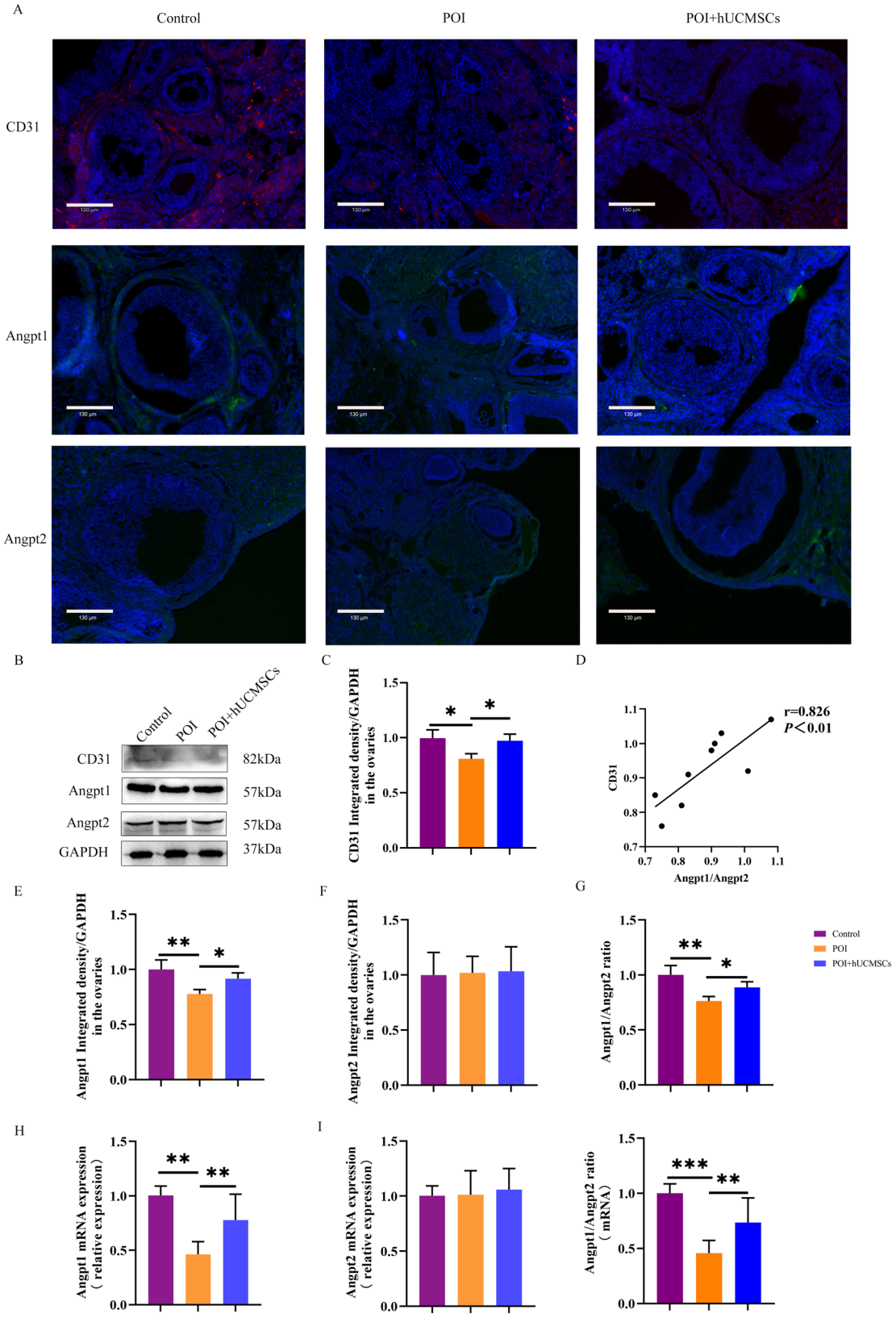


Fig. 4 (See legend on next page.)

(See figure on previous page.)

Fig. 4 hUCMSCs restore ovarian angiogenesis by rebalancing Angpt1/Angpt2 in POI. **A** Immunofluorescence detection of Angpt1, Angpt2 and CD31 expression in the ovaries from control, POI and POI + hUCMSCs group. DAPI repainted nucleus are blue, Angpt1 and Angpt2 positive are green, CD31 positive is red. scale bar is 60 μm. **B** Western blot of CD31, Angpt1, Angpt2, and GAPDH in ovarian tissues across groups. **C**-**E** Quantitative analysis of Angpt1, Angpt2 and CD31(normalized to GAPDH). **F**. The ratio of Angpt1/Angpt2 at protein level. **G**-**I** Quantification of Angpt1, Angpt2 and mRNA expression ratio. **J**. Correlation between Angpt1/Angpt2 protein ratio and CD31 at protein level. Data were shown as mean ± SD of at least three independent experiments. *: $P<0.05$, **: $P<0.01$, ***: $P<0.001$

significantly restored angiogenesis in CTX-damaged ROMECs.

To elucidate the potential mechanism by which hUCMSCs were involved in ROMECs angiogenesis, we analyzed Angpt1 and Angpt2 expression via Western blot and qRT-PCR. Western blot analysis revealed that Angpt1 was dramatically downregulated in CTX-treated ROMECs, whereas Angpt1 expression was upregulated after treatment with hUCMSCs (Angpt1 expression: Control vs. POI: $P=0.019$; POI vs. POI + hUCMSCs: $P=0.008$). However, there were no significant differences in Angpt2 expression across the groups (Fig. 7A-C) (Angpt2 expression: Control vs. POI: $P=0.146$; POI vs. POI + hUCMSCs: $P=0.963$). qRT-PCR revealed that CTX injury reduced Angpt1 mRNA expression, and that hUCMSCs upregulated Angpt1 mRNA expression (Angpt1 mRNA expression: Control vs. POI: $P=0.000$; POI vs. POI + hUCMSCs: $P=0.000$). The mRNA level of Angpt2 remained unchanged across the groups (Fig. 7E, F) (Angpt2 mRNA expression: Control vs. POI: $P=0.503$; POI vs. POI + hUCMSCs: $P=0.527$). In addition, the Angpt1/Angpt2 ratio decreased after CTX

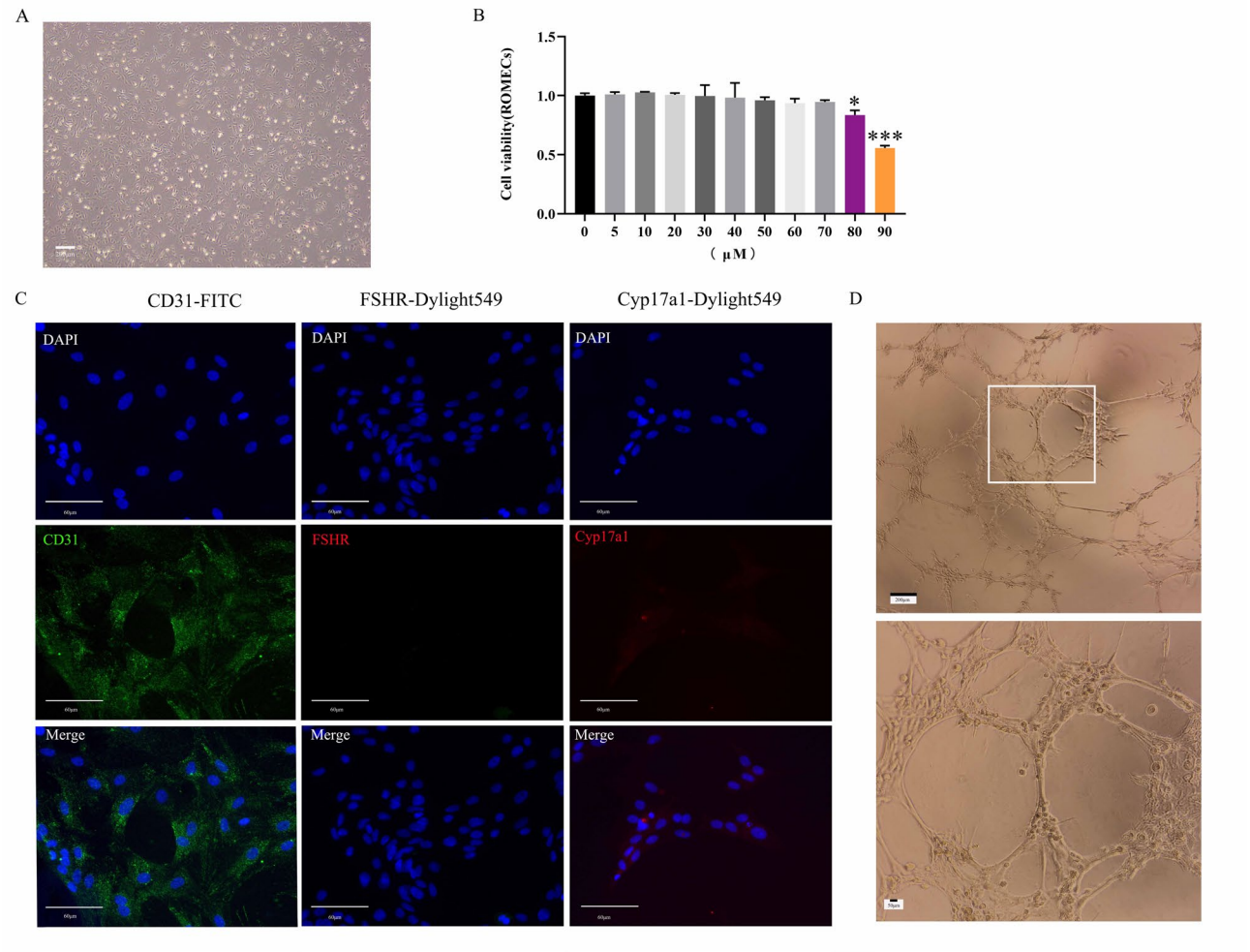


Fig. 5 Isolation and identification of rat ovarian microvascular endothelial cells (ROMECs). **A** Morphology of ROMECs (40×). **B** Viability of ROMECs after CTX treated. **C** Immunofluorescence staining of CD31, FSHR, Cyp17a1 (200×). DAPI is blue and stains the nucleus; CD31 positive is green; FSHR and Cyp17a1 positive are red. **D** Tube formation assay of ROMECs. Data were shown as mean ± SD of at least three independent experiments. *: $P<0.05$, ***: $P<0.001$

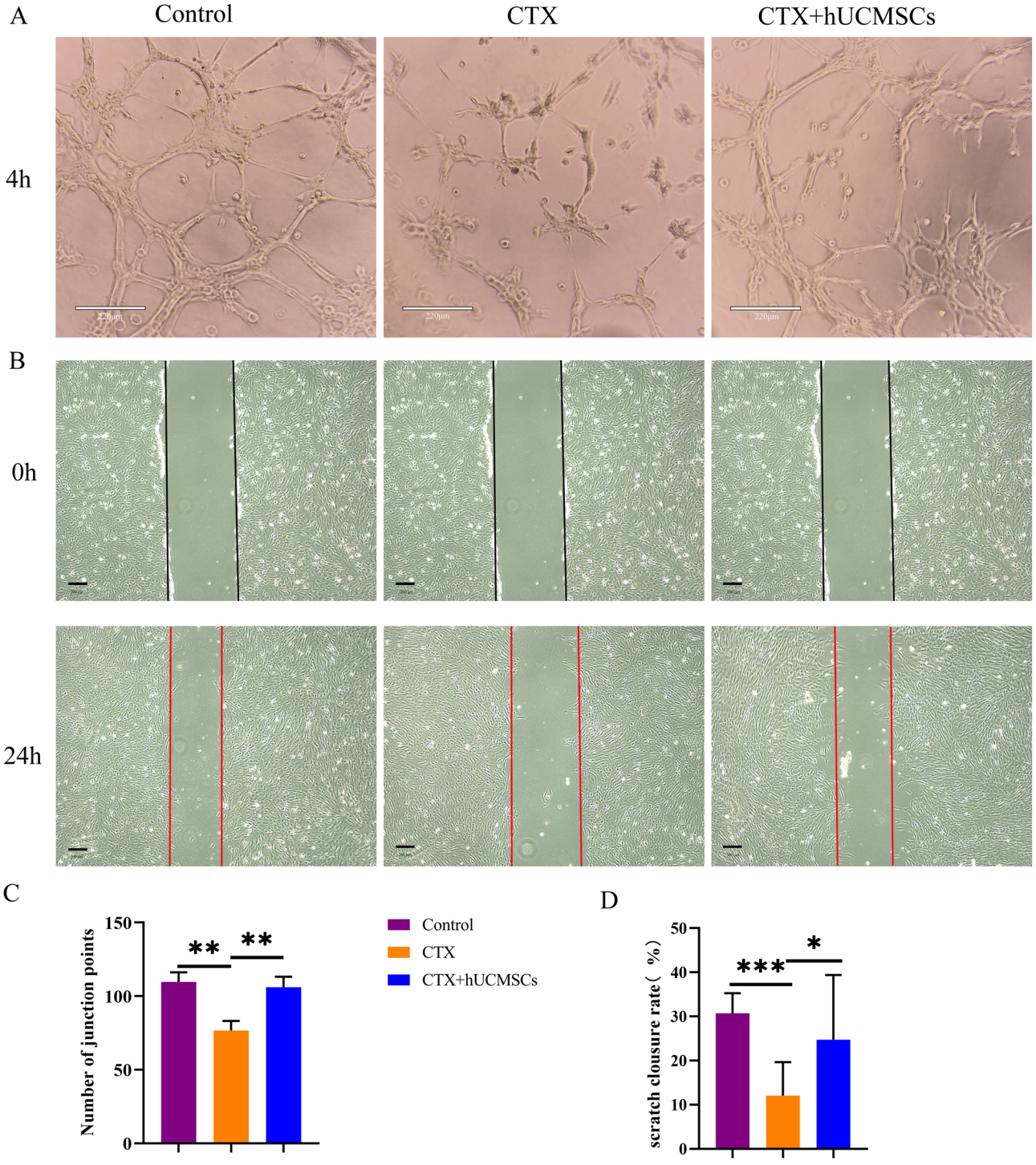


Fig. 6 Effects of CTX and hUCMSCs on angiogenesis in ROMECs. **A** Tube formation assay results after CTX and CTX + hUCMSCs treated. **B** The migration pattern of ROMECs across groups. **C** Quantification of tubule junctions under experimental conditions. **D** Statistical analysis of scratch closure rate. Data were shown as mean ± SD of at least three independent experiments. *: $P<0.05$, **: $P<0.01$, ***: $P<0.001$

exposure but increased after hUCMSCs treatment (Fig. 7D, G) (Angpt1/Angpt2 ratio(protein): Control vs. POI: $P=0.002$, POI vs. POI + hUCMSCs: $P=0.013$; Angpt1/Angpt2 ratio(mRNA): Control vs. POI: $P=0.000$, POI vs. POI + hUCMSCs: $P=0.000$). These results suggested that hUCMSCs rescued CTX-induced angiogenic impairment by regulating the Angpt1/Angpt2 balance.

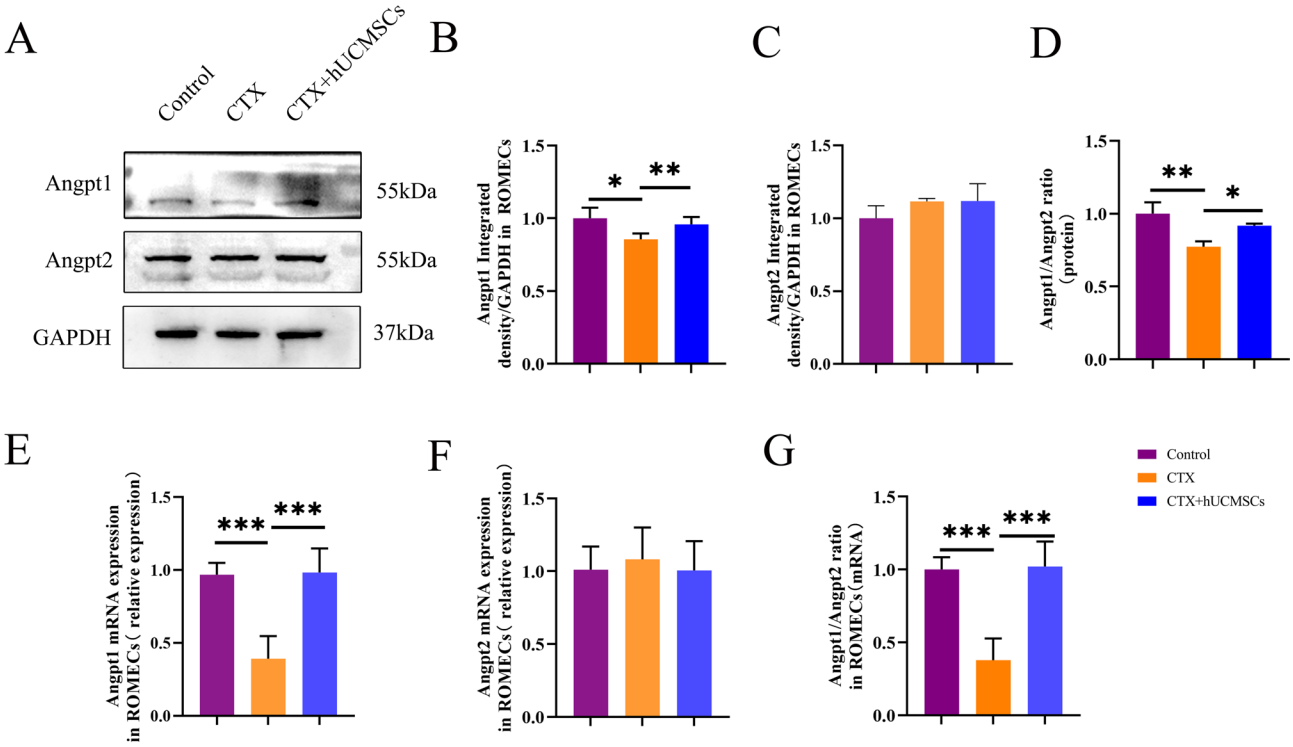


Fig. 7 hUCMSCs Rebalancing the ratio Angpt1/Angpt2 in ROMECs. **A**. Western blot of Angpt1, Angpt2 and GAPDH expression in ROMECs. **B**-**D**. Quantification of Angpt1, Angpt2 protein expression and ratio of Angpt1/Angpt2. **E**-**J**. qRT-PCR analysis of Angpt1, Angpt2 and the ratio Angpt1/Angpt2 at mRNA level. Data were shown as mean ± SD of at least three independent experiments. *: $P<0.05$, **: $P<0.01$, ***: $P<0.001$

Discussion

This study established a POI rat model via the intraperitoneal injection of cyclophosphamide. After treatment with hUCMSCs, the weights of the body and ovaries, the numbers of growing follicles and the hormone levels of the rats significantly improved. These findings suggested that hUCMSCs could restore ovarian function in POI rats, but the specific mechanism remains unclear.

Numerous studies had shown that MSCs could improve follicle development and sex hormone secretion in POI, repair ovarian function, and increase fertility [34–38]. However, studies on the relationship between MSCs and the ovarian vascular system had rarely been reported. In this work, GFP-labeled hUCMSCs were injected into rats, and the results revealed that the hUCMSCs homed to the theca layers. VEGF and CD31 were reduced in POI rats, and significantly increased after treatment with hUCMSCs. In vitro experiments revealed that hUCMSCs significantly promoted the migration and lumen formation of CTX-damaged ROMECs. These findings indicated that the vascular network was disrupted and that accelerated follicular attrition, after hUCMSCs treatment could reconstitute the vascular architecture to promote follicular growth and restore ovarian function.

Through bioinformatics analysis, we screened Angpt1 as a hub gene for cell migration and angiogenesis. Moreover, Angpt1 was downregulated and Angpt2 as not changed in the POI group. Therefore, we postulated that imbalances in Angpt1 and Angpt2 influenced the cell migration and angiogenesis and that hUCMSCs could enhance ovarian function through controlling the balance of Angpt1 and Angpt2.

Angpt1 and Angpt2 were essential members of the angiopoietin family and played critical roles in angiogenesis regulation. Angpt1 was involved in vascular maturation, stability, and remodeling and increased endothelial cell migration and survival [39]. In contrast, Angpt2 acted as a natural antagonist of Angpt1, promoting vascular remodeling in the presence of VEGF and inducing vascular regression in the absence of VEGF [40]. Previous studies had shown that both Angpt1 and Angpt2 were associated with folliculogenesis in rats [41]. The Angpt1/Angpt2 ratio was associated with PCOS in patients [42]. In a PCOS rat model followed by DHEA injection, Angpt1 was upregulated, and Angpt2 was downregulated [43].

Our results revealed that the expression of Angpt1 was significantly reduced in the POI group but increased in the hUCMSCs-treated group. In contrast, Angpt2 expression remained stable across all groups. Consequently, the Angpt1/Angpt2 ratio decreased markedly in the POI group and increased after hUCMSCs therapy. The ratio was positively correlated with the expression of CD31. In vitro findings demonstrated a parallel trend

in ROMECs. Treatment with CTX significantly downregulated Angpt1 expression, whereas Angpt2 levels remained unaltered, resulting in a reduced Angpt1/Angpt2 ratio. Conversely, subsequent hUCMSCs therapy reversed this imbalance, elevating Angpt1 expression and restoring the Angpt1/Angpt2 ratio. Our data demonstrated that dysregulation of the Angpt1/Angpt2 axis was involved in ovarian vascular dysfunction in POI, and that hUCMSCs could modulate vascular homeostasis to restore ovarian function. Our in vitro co-culture system demonstrated an indirect functional impact on ROMECs, indicating that the contribution of paracrine signaling to the ovarian microenvironment. The paracrine pathway was recognized as a key mechanism through which MSCs ameliorated ovarian injury and enhanced ovarian function [44–47]. However, this mechanism needs further investigation.

Our study has several limitations that should be considered. First, the analyses were primarily performed at a single time point post-treatment, which may not fully capture dynamic processes such as vascular remodeling and vascular permeability, both of which are regulated by angiopoietins. Second, functional fertility outcomes were not evaluated, as mating trials were not conducted to directly assess reproductive restoration. These limitations provide a roadmap for future research directions.

In future studies, we will address these limitations by employing exosome experiments, multiple time-point analyses, vascular permeability assays, and functional fertility tests. Furthermore, techniques such as single-cell sequencing and follicle culture approaches will be utilized to clarify the precise cellular targets and molecular cascades involved in how hUCMSCs restore ovarian function in POI.

Conclusions

Our integrated in vivo and in vitro studies demonstrated that hUCMSCs could rebalance the Angpt1/Angpt2 axis, thereby promoting angiogenesis and improving ovarian function in CTX-induced POI model rats. Specifically, hUCMSCs home to ovarian theca-interstitial layers while normalizing the Angpt1/Angpt2 ratio. These findings establish angiopoietin ratio modulation as a therapeutic mechanism, providing a foundation for the clinical translation foundation of hUCMSCs therapies that target POI.

Supplementary Information

The online version contains supplementary material available at https://doi.org/10.1186/s13048-025-01856-3.

Supplementary Material 1.

Supplementary Material 2.

Acknowledgements

We would like to thank the developers of BioGDP for providing graphical abstract resources and Sangerbox for its valuable tools in data visualization.

Authors' contributions

Qianqian Luo, Ranran Liu and Zhonglin Jiang: Reagents, materials, analysis tools or data; Yongtao Su, Ranran Liu: Conceived and designed the experiments; Qianqian Luo, Chengen Liu and Zhonglin Jiang: Wrote the paper, conceived and designed the experiments, performed the experiments and analyzed and interpreted the data.Qianqian Luo and Chengen Liu contributed equally to this work and shared the first authorship. Corresponding author: Corresponding author: Zhonglin Jiang, Yongtao Su and Ranran Liu.

Funding

This research was supported by the Natural Science Foundation of Shandong Province (ZR2022MH097, ZR2021QH149, ZR2022QC082) and the TCM Science and Technology Project of Shandong Province(Q2023057).

Data availability

The data will be made available upon reasonable request from the corresponding author.

Declarations

Ethics approval and consent to participate

The study was approved by the Medical Ethics Committee of Binzhou Medical University (ethics number 2022 – 315). All applicable institutional and national guidelines for the care and use of animals were followed.

Consent for publication

All authors gave consent for publication.

Competing interests

The authors declare no competing interests.

Received: 8 August 2025 / Accepted: 8 October 2025
Published online: 18 November 2025

References

1. Baerwald AR, Adams GP, Pierson RA. Ovarian antral folliculogenesis during the human menstrual cycle: a review. Hum Reprod Update. 2012;18(1):73–91.
2. Ke HN, Tang SY, Guo T, Hou D, Jiao X, Li S, et al. Landscape of pathogenic mutations in premature ovarian insufficiency. Nat Med. 2023;29(2):483–92.
3. Luisi S, Orlandini C, Regini C, Pizzo A, Vellucci F, Petraglia F. Premature ovarian insufficiency: from pathogenesis to clinical management. J Endocrinol Invest. 2015;38(6):597–603.
4. Panay PN, Anderson RA, Bennie A, Cedars M, Davies M, Ee C, et al. Evidence-based guideline: premature ovarian insufficiency. Hum Reprod Open. 2024;2024(4):hoae065.
5. Mason JB, Habermehl TL, Underwood KB, Schneider A, Brieño-Enriquez MA, Masternak MM, et al. The interrelationship between female reproductive aging and survival. The Journals of Gerontology: Series A. 2022;77(1):75–83.
6. Mishra GD, Pandeya N, Dobson AJ, Chung HF, Anderson D, Kuh D, Sandin S, Giles GG, Bruinsma F, Hayashi K, Lee JS, Mizunuma H, Cade JE, Burley V, Greenwood DC, Goodman A, Simonsen MK, Adami HO. Demakakos P,Weiderpass E. Early menarche, nulliparity and the risk for premature and early natural menopause. Hum Reprod. 2017;32(3):679–86.
7. Li M, Zhu Y, Wei J, Chen L, Chen S, Lai D. The global prevalence of premature ovarian insufficiency: a systematic review and meta-analysis. Climacteric. 2023;26(2):95–102.
8. Huhtaniemi I, Hovatta O, La Marca A, Livera G, Monniaux D, Persani L, et al. Advances in the molecular pathophysiology, genetics, and treatment of primary ovarian insufficiency. Trends Endocrinol Metab. 2018;29(6):400–19.
9. Nie L, Wang X, Wang S, Hong Z, Wang M. Genetic insights into the complexity of premature ovarian insufficiency. Reprod Biol Endocrinol. 2024;22(1):94.
10. Jinno M. Ovarian stimulation by promoting basal follicular growth. Reprod Biol Endocrinol. 2025;23(1):35.

11. Zhang T, He M, Zhang J, Tong Y, Chen T, Wang C, et al. Mechanisms of primordial follicle activation and new pregnancy opportunity for premature ovarian failure patients. Front Physiol. 2023;14:1113684.
12. Dou XQ, Jin X, Chen XB, Zhou Q, Chen HY, Wen MX, et al. Bu-Shen-Ning-Xin Decoction alleviates premature ovarian insufficiency (POI) by regulating autophagy of granule cells through activating PI3K/AKT/mTOR pathway. Gynecol Endocrinol. 2022;38(9):754–64.
13. Wang FX, Liu YF, Ni FD, Jin JN, Wu YQ, Huang Y, et al. BNC1 deficiency-triggered ferroptosis through the NF2-YAP pathway induces primary ovarian insufficiency. Nat Commun. 2022;13(1):5871.
14. Gao M, Zhang T, Chen T, Chen Z, Zhu Z, Wen Y, et al. Polycomb repressive complex 1 modulates granulosa cell proliferation in early folliculogenesis to support female reproduction. Theranostics. 2024;14(4):1371–89.
15. Shao T, Ke H, Liu R, Xu L, Han S, Zhang X, Dang Y, Jiao X, Li W, J Chen Z, Qin Y, Zhao S. Autophagy regulates differentiation of ovarian granulosa cells through degradation of WT1. Autophagy. 2022;18(8):1864–78.
16. Akiyama I, Yoshino O, Osuga Y, Shi J, Harada M, Koga K, et al. Bone morphogenetic protein 7 increased vascular endothelial growth factor (VEGF)-A expression in human granulosa cells and VEGF receptor expression in endothelial cells. Reprod Sci. 2014;21(4):477–82.
17. Robinson RS, Woad KJ, Hammond AJ, Laird M, Hunter M, G,Mann GE. Angiogenesis and vascular function in the ovary. Reproduction. 2009;138(6):869–81.
18. Scotti L, Abramovich D, Pascuali N, Durand LH, Irusta G, de Zúñiga I, Tesone M, Parborell F. Inhibition of angiopoietin-1 (ANGPT1) affects vascular integrity in ovarian hyperstimulation syndrome (OHSS). Reprod Fertil Dev. 2016;28(6):690–9.
19. Parborell F, Abramovich D, Irusta G, Tesone M. Angiopoietin 1 reduces rat follicular atresia mediated by apoptosis through the PI3K/Akt pathway. Mol Cell Endocrinol. 2011;343(1–2):79–87.
20. Parborell F, Abramovich D, Tesone M. Intrabursal administration of the antiangiopoietin 1 antibody produces a delay in rat follicular development associated with an increase in ovarian apoptosis mediated by changes in the expression of BCL2 related genes. Biol Reprod. 2008;78(3):506–13.
21. Ahmadian S, Sheshpari S, Pazhang M, Bedate AM, Beheshti R, Abbasi MM, et al. Intra-ovarian injection of platelet-rich plasma into ovarian tissue promoted rejuvenation in the rat model of premature ovarian insufficiency and restored ovulation rate via angiogenesis modulation. Reprod Biol Endocrinol. 2020;18(1):78.
22. Nishigaki A, Okada H, Tsuzuki T, Cho H, Yasuda K, Kanzaki H. Angiopoietin 1 and angiopoietin 2 in follicular fluid of women undergoing a long protocol. Fertil Steril. 2011;96(6):1378–83.
23. Di Pietro M, Parborell F, Irusta G, Pascuali N, Bas D, Bianchi MS, et al. Metformin regulates ovarian angiogenesis and follicular development in a female polycystic ovary syndrome rat model. Endocrinology. 2015;156(4):1453–63.
24. Sullivan SD, Sarrel PM, Nelson LM. Hormone replacement therapy in young women with primary ovarian insufficiency and early menopause. Fertil Steril. 2016;106(7):1588–99.
25. Lambertini M, Horicks F, Del Mastro L, Partridge A, H,Demeestere I. Ovarian protection with gonadotropin-releasing hormone agonists during chemotherapy in cancer patients: from biological evidence to clinical application. Cancer Treat Rev. 2019;72:65–77.
26. Dai W, Xu B, Ding L, Zhang Z, Yang H, He T, et al. Human umbilical cord mesenchymal stem cells alleviate chemotherapy-induced premature ovarian insufficiency mouse model by suppressing ferritinophagy-mediated ferroptosis in granulosa cells. Free Radic Biol Med. 2024;220:1–14.
27. Shuyuan Y, Meimei W, Fenghua L, Huishan Z, Min C, Hongchu B, et al. hUMSC transplantation restores follicle development in ovary damaged mice via re-establish extracellular matrix (ECM) components. J Ovarian Res. 2023;16(1):172.
28. Cui L, Bao H, Zhu W, Tang Y, Luo Q, Si Y, et al. hUMSCs transplantation regulates AMPK/NR4A1 signaling axis to inhibit ovarian fibrosis in POI rats. Stem Cell Rev Rep. 2023;19(5):1449–65.
29. Luo Q, Tang Y, Jiang Z, Bao H, Fu Q, Zhang H. hUCMSCs reduce theca interstitial cells apoptosis and restore ovarian function in premature ovarian insufficiency rats through regulating NR4A1-mediated mitochondrial mechanisms. Reprod Biol Endocrinol. 2022;20(1):125.
30. Sakurai T, Suzuki K, Yoshie M, Hashimoto K, Tachikawa E, Tamura K. Stimulation of tube formation mediated through the prostaglandin EP2 receptor in rat luteal endothelial cells. J Endocrinol. 2011;209(1):33–43.
31. Pusztaszeri MP, Seelentag W, Bosman FT. Immunohistochemical expression of endothelial markers CD31, CD34, von Willebrand factor, and Fli-1 in normal human tissues. J Histochem Cytochem. 2006;54(4):385–95.
32. Tang Y, He Y, Huo X, Chen J, Qian M, Huang H, et al. HUMSC-derived exosomes alleviate follicular interstitial cell autophagy by let-7a-5p/AMPK/mTOR axis in POI rats. Stem Cell Res Ther. 2025;16(1):291.
33. Chen J, Huo X, Qian M, Xue Q, He Y, Xu P, et al. Exosomes derived from human mesenchymal stem cells mitigate follicular interstitial cell ferroptosis via the miR-26a-5p/PTEN/GPX4 axis in rats with chemotherapy-induced premature ovarian insufficiency. Int J Nanomed. 2025;20:10195–212.
34. Cao RC, Lv Y, Lu G, Liu HB, Wang WM, Tan CL, et al. Extracellular vesicles from iPSC-MSCs alleviate chemotherapy-induced mouse ovarian damage via the ILK-PI3K/AKT pathway. Zool Res. 2023;44(3):620–35.
35. Zhang SH, Yahaya BH, Pan Y, Liu Y, L,Lin JT. Menstrual blood-derived endometrial stem cell, a unique and promising alternative in the stem cell-based therapy for chemotherapy-induced premature ovarian insufficiency. Stem Cell Res Ther. 2023;14(1):327.
36. Ling L, Hou JY, Liu DN, Tang DY, Zhang YQ, Zeng QR, Pan H, Fan L. Important role of the SDF-1/CXCR4 axis in the homing of systemically transplanted human amnion-derived mesenchymal stem cells (hAD-MSCs) to ovaries in rats with chemotherapy-induced premature ovarian insufficiency (POI). Stem Cell Res Ther. 2022;13(1):79.
37. Ling L, Feng X, Wei T, Wang Y, Wang Y, Wang Z, et al. Human amnion-derived mesenchymal stem cell (hAD-MSC) transplantation improves ovarian function in rats with premature ovarian insufficiency (POI) at least partly through a paracrine mechanism. Stem Cell Res Ther. 2019;10(1):46.
38. Ling L, Feng X, Wei T, Wang Y, Wang Y, Zhang W, et al. Effects of low-intensity pulsed ultrasound (LIPUS)-pretreated human amnion-derived mesenchymal stem cell (hAD-MSC) transplantation on primary ovarian insufficiency in rats. Stem Cell Res Ther. 2017;8(1):283.
39. Davis S, Aldrich TH, Jones PF, Acheson A, Compton DL, Jain V, et al. Isolation of angiopoietin-1, a ligand for the TIE2 receptor, by secretion-trap expression cloning. Cell. 1996;87(7):1161–9.
40. Gale NW, Thurston G, Hackett SF, Renard R, Wang Q, McClain J, Martin C, Witte C, Witte MH, Jackson D, Suri C, Campochiaro PA, Wiegand S. J,Yancopoulos G D. Angiopoietin-2 is required for postnatal angiogenesis and lymphatic patterning, and only the latter role is rescued by Angiopoietin-1. Dev Cell. 2002;3(3):411–23.
41. Abramovich D, Rodriguez Celin A, Hernandez F, Tesone M, Parborell F. Spatio-temporal analysis of the protein expression of angiogenic factors and their related receptors during folliculogenesis in rats with and without hormonal treatment. Reproduction. 2009;137(2):309–20.
42. Scotti L, Parborell F, Irusta G, De Zuñiga I, Bisioli C, Pettorossi H, et al. Platelet-derived growth factor BB and DD and angiopoietin1 are altered in follicular fluid from polycystic ovary syndrome patients. Mol Reprod Dev. 2014;81(8):748–56.
43. Abramovich D, Irusta G, Bas D, Cataldi NI, Parborell F, Tesone M. Angiopoietins/TIE2 system and VEGF are involved in ovarian function in a DHEA rat model of polycystic ovary syndrome. Endocrinology. 2012;153(7):3446–56.
44. Wang Z, Wang Y, Yang T, Li J, Yang X. Study of the reparative effects of menstrual-derived stem cells on premature ovarian failure in mice. Stem Cell Res Ther. 2017;8(1):11.
45. Liu J, Zhang H, Zhang Y, Li N, Wen Y, Cao F, et al. Homing and restorative effects of bone marrow-derived mesenchymal stem cells on cisplatin injured ovaries in rats. Mol Cells. 2014;37(12):865–72.
46. Song D, Zhong Y, Qian C, Zou Q, Ou J, Shi Y, et al. Human umbilical cord mesenchymal stem cells therapy in cyclophosphamide-induced premature ovarian failure rat model. BioMed Res Int. 2016;2016:2517514.
47. Zhang Q, Bu S, Sun J, Xu M, Yao X, He K, et al. Paracrine effects of human amniotic epithelial cells protect against chemotherapy-induced ovarian damage. Stem Cell Res Ther. 2017;8(1):270.

Publisher's Note

Springer Nature remains neutral with regard to jurisdictional claims in published maps and institutional affiliations.